


Cite this: *RSC Adv.*, 2024, 14, 21945

# Greener solvents for the processing of preceramic polycarbosilane: application in the preparation of B<sub>4</sub>C/SiC composites†

Marion Weissenberger,<sup>ab</sup> Adrien Vincent,<sup>b</sup> Yves Champavier,<sup>c</sup> Cristina Coelho Diogo,<sup>d</sup> Florence Babonneau,<sup>e</sup> Nicolas Pradeilles,<sup>a</sup> Alexandre Maître<sup>a</sup> and Romain Lucas-Roper<sup>\*a</sup>

The innovation introduced in this study consists of replacing toluene with safer solvents such as cyclopentane or diethyl ether in the processing of a preceramic polycarbosilane (allylhydridopolycarbosilane, AHPCS) and assessing its impact on the functionalisation of B<sub>4</sub>C powders to produce B<sub>4</sub>C/SiC composites. Fourier-transform infrared (FT-IR) with ATR and nuclear magnetic resonance (NMR) spectroscopy revealed no major modification in the polymer structure. SEC/MALS analysis showed a slight change in the number-average molar mass of the polymer regardless of the functionalisation solvent used in correlation with a slight decrease in the polymer ceramic yield due to oligomer loss. The thermal behaviour of the preceramic polymer investigated *via* mass spectrometry remained unaffected by the solvent change. The search for polymer residues after distillation highlighted the recyclability of both the functionalisation solvent and the polymer, despite a slight increase in the molar mass of the polymer. Finally, the sinterability of B<sub>4</sub>C/AHPCS samples was studied with the preparation of B<sub>4</sub>C/SiC composites *via* a polymer-derived ceramic (PDC) route and spark plasma sintering (SPS). The effect of the solvent on the microstructure and relative density of the specimens (>92%) is negligible. The specimens retain a fine and homogeneous phase distribution despite process modification. The results highlight the approach developed to use greener solvents for the chemical synthesis of functionalised ceramics and represent a step towards the generalisation of more environmentally friendly processes.

Received 17th June 2024  
Accepted 27th June 2024

DOI: 10.1039/d4ra04431b

rsc.li/rsc-advances

## Introduction

Nowadays, the processes for producing non-oxide ceramics are constantly evolving in order to modulate the microstructure properties (*e.g.* relative density and phase distribution) and define the thermophysical features (hardness, electrical or thermal conductivity) of the materials.<sup>1,2</sup> The polymer-derived ceramic (PDC) strategy has proved to be a good way for modulating the ceramic composition or microstructure in order to obtain desired properties.<sup>3,4</sup> Indeed, the PDC route consists of using a polymer as a ceramic precursor, which becomes

a ceramic material after pyrolysis and crystallisation. Among the ceramic precursors, polycarbosilanes are commonly used for their ability to generate SiC-based ceramics with a wide range of applications in the additive manufacturing field,<sup>5–7</sup> shaping of the membrane,<sup>8,9</sup> and for bulk material production.<sup>10–12</sup> Among all the silicon-based preceramic polymers, allylhydridopolycarbosilane (AHPCS), also known as SMP-10 (StarPCS SMP-10, Starfire Systems, USA), has attracted growing interest from the scientific community, with nearly 300 references in publications since 2015. This polymer is of great interest because its Si/C ratio is close to one, leading to a nearly stoichiometric SiC ceramic after pyrolysis with a low amount of residual carbon. The ceramic yield of a preceramic polymer is also an important parameter to estimate the amount of the polymer needed to produce the desired amount of specimen, keeping in mind the volume shrinkage during material processing. This polymer has an interesting ceramic yield (near 70%)<sup>11,13,14</sup> that can be modulated *via* chemical and/or heat treatment for cross-linking activation. Moreover, polymer composition can easily be adjusted by introducing metallic elements.<sup>15</sup> In addition, its viscosity is suitable for shaping processes, especially for 3D manufacturing purposes.<sup>16</sup>

<sup>a</sup>University of Limoges, IRCER, UMR 7315, Limoges, F-87068, France. E-mail: romain.lucas@unilim.fr

<sup>b</sup>Saint-Gobain Research Provence, Cavaillon, F-84306, France

<sup>c</sup>Univ. Limoges, CNRS, Inserm, CHU Limoges, BISCeM, UAR 2015, US 42, Limoges, F-87068, France










<sup>d</sup>FCMat, Fédération de Chimie et Matériaux de Paris Centre, CNRS, Sorbonne Université, FR2482, Paris, F-75005, France

<sup>e</sup>Laboratoire de Chimie de la Matière Condensée de Paris (LCMCP), CNRS, Sorbonne Université, UMR 7574, Campus Jussieu, 4 Place Jussieu, Paris, F-75005, France

† Electronic supplementary information (ESI) available. See DOI: <https://doi.org/10.1039/d4ra04431b>



**Table 1** Solvents commonly used to solubilise AHPCS (top section) and a list of candidates to replace them (bottom section) with their associated permittivity ( $\epsilon$ ), dipole moment ( $\mu$ ), Hansen solubility parameters and boiling temperature<sup>11,12,17–21</sup>

Solvent	Pictograms	$\epsilon$ (F m <sup>-1</sup> )	$\mu$ (C m <sup>-1</sup> )	Hansen solubility parameters (MPa <sup>0.5</sup> )				Boiling temperature (°C)
				$\delta_{\text{tot}}$	$\delta_{\text{D}}$	$\delta_{\text{P}}$	$\delta_{\text{H}}$	
Toluene		2.38	0.31	18.2	18	1.4	2.0	110.6
Cyclohexane		1.9	0	16.8	16.8	0	0.2	81
Hexane		1.88	0.08	14.9	14.9	0	0	69
Pentane		1.84	0	14.5	14.5	0	0	36.1
Tetrahydrofuran (THF)		7.58	1.69	19.5	16.8	5.7	8.0	66
Acetic acid		6.15	1.68	21.4	14.5	8	13.5	118
Cyclopentane		1.97	0	16.4	16.4	0	1	49.2
Diethyl ether		4.33	1.3	15.5	14.5	2.9	4.6	34.6
TMO 2,2,5,5-tetramethyloxolane		5.03	1.86	15.7	15.4	2.4	2.1	112

However, in many processes, handling such hydrophobic polycarbosilane requires organic solvents for solubilization or dissolution. Table 1 (top section) lists the solvents commonly used to dissolve AHPCS and highlights the danger and toxicity of these solvents. Faced with this situation, this study aims to find a greener solvent in order to replace those commonly used with AHPCS, *i.e.*, toluene, cyclohexane and tetrahydrofuran, that are highly toxic. This innovative approach has never been previously reported in the literature for polymers in order to produce ceramics. Driven by the principles of Green chemistry, the new solvent is required to be miscible with AHPCS. In this way, the miscibility criteria will be considered to establish a selection of solvent candidates to replace toluene, one of the most frequently used solvents for AHPCS dissolution.<sup>6,17,22,23</sup> After being in contact with the solvent, the structure of the polymer and its recyclability will be investigated. Finally, the impact of the replacement solvent will be illustrated with the sintering ability of B<sub>4</sub>C ceramic powders functionalised with AHPCS.

## Experimental

### Raw chemicals and powders

Commercially available allylhydridopolycarbosilane (AHPCS) was used as received (Starfire Systems Inc., USA). The structure

of the preceramic polymer provided by the supplier is presented in Fig. 1. This molecular structure was investigated and confirmed by NMR spectroscopy. The solvents used in this study included toluene (laboratory reagent grade-Fisher Scientific), diethyl ether and cyclopentane (Sigma Aldrich Chimie, France), and acetic acid (99.5% pure-Acros Organics), which were designated as T, D, C and A, respectively. Boron carbide powder (ABCR GmbH, grade HD20) with a mean particle size ranging between 0.3 and 0.6  $\mu\text{m}$  was used for the functionalisation.

### Miscibility tests

Miscibility tests between the polymer and solvent were performed by mixing 2.5 mL of solvent with 30  $\mu\text{L}$  of polymer at

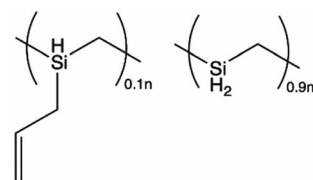


**Fig. 1** AHPCS (SMP-10, Starfire Systems) structure confirmed by the literature.<sup>14</sup>



room temperature in a small glass tube. These polymer/solvent proportions were used in a previous study, and were adapted here for the functionalisation of B<sub>4</sub>C powders.<sup>11</sup> The miscibility was validated by a visual test (positive: one phase; negative: two phases) immediately after stirring the mixture and after 5 minutes of rest.

### Characterisation

The polymer that was in contact with a solvent will be named **AHPCS-T**, **D** or **C**. Regarding the solvents that have been in contact with the polymer, they will be named as follows: **T**-, **D**- or **C**-**AHPCS**.

### Fourier-transform infrared (FT-IR (ATR)) spectroscopy

FT-IR spectroscopy analysis was carried out in transmission mode (4000–400 cm<sup>−1</sup>, Nicolet iS10-Thermo Scientific software: Omnic).

FT-IR (ATR) (cm<sup>−1</sup>) for **AHPCS**, **AHPCS-T**, **D** and **C**:  $\nu(\text{C-H})$ : 2840–3000; 3078,  $\nu(\text{Si-H})$ : 2130,  $\nu(\text{C=O})$ : 1631,  $\delta(\text{C-H})$ : 1356,  $\nu(\text{Si-CH}_3)$ : 1255,  $\delta(\text{Si-CH}_2\text{-Si})$ : 1046,  $\delta(\text{Si-H})$ : 939,  $\nu(\text{Si-C})$ : 856,  $\delta(\text{Si-CH}_3)$ : 766. **T-AHPCS**:  $\nu(\text{C-H, aromatic})$ : 2856–3102,  $\delta(\text{C-H})$ : 1027; 1080. **D-AHPCS**:  $\nu(\text{C-H})$ : 2870; 2976,  $\delta(\text{CH}_3)$ : 1351; 1383. **C-AHPCS**:  $\nu(\text{C-H})$ : 2874; 2954.

### Nuclear magnetic resonance (NMR) spectroscopy

<sup>1</sup>H and <sup>13</sup>C liquid-state NMR spectra were recorded on a Bruker Avance III HD 500 MHz spectrometer. Analyses were performed in toluene-d<sub>8</sub>.

<sup>1</sup>H NMR (ppm) **AHPCS**, **AHPCS-T**, **D** and **C** (toluene-d<sub>8</sub>):  $\delta$ : 4.96–5.75 (CH=CH<sub>2</sub>),  $\delta$ : 3.73–4.12 (Si-H),  $\delta$ : 1.36–1.60 (Si-CH<sub>2</sub>),  $\delta$ : −0.3–0.08 (Si-CH<sub>3</sub>). <sup>13</sup>C NMR (ppm) **AHPCS**, **AHPCS-T**, **D** and **C** (toluene-d<sub>8</sub>):  $\delta$ : 50–70, 114 and 130 (CH=CH<sub>2</sub> allyl carbons),  $\delta$ : <0 (Si-CH<sub>3</sub>).

<sup>29</sup>Si liquid-state NMR spectra were recorded on a Bruker Avance 500 MHz spectrometer in chloroform-d.

<sup>29</sup>Si NMR (ppm) **AHPCS**, **AHPCS-T**, **D** and **C** (CDCl<sub>3</sub>):  $\delta$ : −8 to −15 (C<sub>3</sub>SiH),  $\delta$ : −30 to −40 (C<sub>2</sub>SiH<sub>2</sub>),  $\delta$ : −60 to −67 (CSiH<sub>3</sub>).

### Thermogravimetric analysis coupled with mass spectrometry (TGA-MS)

The thermal behaviour of the polymer was analysed using thermogravimetric equipment (STA 449F3-Netzsch) associated with a mass spectrometer (Omnistar, Balzers Instrument) with a heating ramp of 10 °C min<sup>−1</sup> up to 1400 °C under argon flow.

### Size-exclusion chromatography combined with multi-angle light scattering (SEC-MALS)

The determination of the molecular weight of the polymer was carried out using size-exclusion chromatography combined with multi-angle light scattering (SEC-MALS). The molar mass/conformation analysis of the polymer solutions as carried out using a size-exclusion chromatography system from Shimadzu (LC20AD pump, CTO-20AC oven and SPD-20A detector), coupled to a DAWN HELEOS II detector (MALS) with an Optilab T-REX refractometer, both from Wyatt. The solvent used was

toluene, and a dn/dc of 0.0528 mL g<sup>−1</sup> for AHPCS was obtained beforehand.

### Preparation of the mixture (polymer/solvent) and evaporation of the solvent

The polymer was mixed with the solvent under stirring for 24 hours at room temperature. The solvent was then extracted with a rotary evaporator (pump: C 3001 Vario pro-Vacuum brand; heating bath and rotation device-Heidolph). No heating was required to evaporate **D** and **C**. **T** was extracted with a heating bath set at 45 °C, and the extraction lasted between one and two hours. The extraction for **D** and **C** proceeded with several evaporation stages from 970 to 5 mbar, and lasted between one and two hours. These intermediary stages were settled in order to adjust the extraction speed and recover as much solvent as possible.

### Sintering and specimen characterisation

The functionalised B<sub>4</sub>C powder was sintered in a 20 mm graphite die using spark plasma sintering (Dr Sinter 825, Syntex, Japan).<sup>24</sup> Crystalline phases were identified by X-ray diffraction analyses using Cu K $\alpha_{1,2}$  radiation for angles ( $2\theta$ ) ranging between 10° and 120°, with a LYNXEYE XE-T detector (D8 advance, Bruker, Wissembourg, France). Transmission electron microscopy (JEOL-2100 F, Tokyo, Japan) images were recorded to characterise the structural properties of the elemental particles and their morphology before and after functionalisation. Scanning electron microscopy (FEG-SEM Quanta 450, FEI, Thermo Fisher Scientific, USA) studies were carried out to observe the microstructure of the sintered samples. The relative densities of the specimens were determined by Archimedes method with absolute ethanol, whose density was adjusted depending on the temperature during measurements. Relative density values result from the ratio between the density measured by Archimedes method and the theoretical density calculated on the basis of a law of mixture.

## Results and discussion

### Towards greener solvents

Two main specifications were taken into consideration to select greener solvents for the processing of **AHPCS**. The first concerned the miscibility between the polymer and the solvent, and the second was the hazardous nature of the reagents used in the process. Some physical indicators of solubility such as the Hansen solubility parameters (HSP) seemed to be a good way of predicting the miscibility behaviour of the solvent with respect to the polymer.<sup>19,25</sup> In addition, the physicochemical parameters of solvents, such as permittivity or dipole moment, also appeared to be relevant in predicting the possible miscibility between two species.<sup>26,27</sup> Table 1 contains a list of potential solvents for the replacement of toluene.

This list was based on the most widely available and used solvents. The selection was made by excluding solvents bearing a “Serious health hazard” pictogram. A second criterion was taken into account to select solvents with HSP, permittivity, or

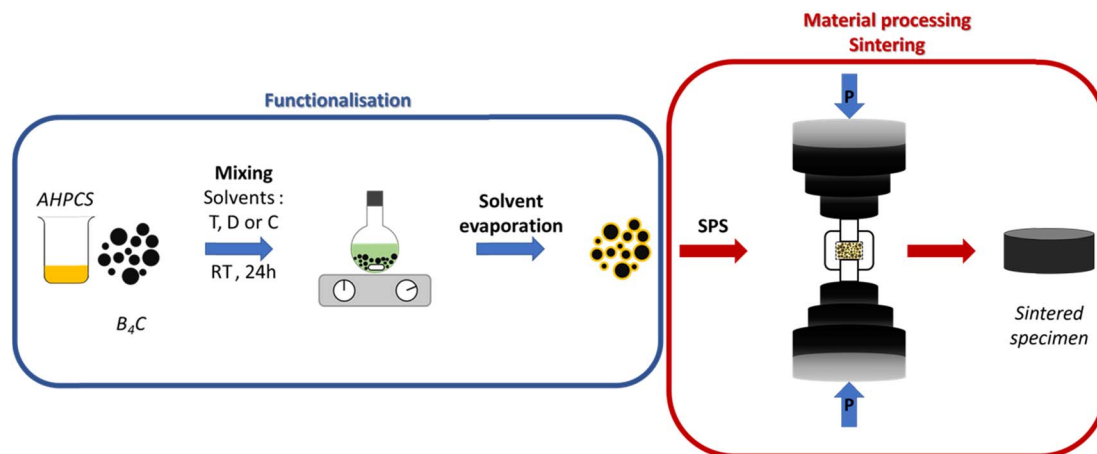


Fig. 2 General protocol for the functionalisation of the  $B_4C$  particle with AHPCS, followed by sintering (T = toluene; D = diethyl ether; C = cyclopentane).

dipole moment that was close to toluene. Limits have been set regarding the permittivity ( $<7$ ), dipole moment ( $<2$ ), and HSP (between 14 and 22). With these criteria, four candidates were selected to replace toluene (T): acetic acid (A), diethyl ether (D), cyclopentane (C) and tetramethyloxolane (TMO). The latter was withdrawn from the selection for economic reasons and due to its low availability (600 € for 250 mg).<sup>28</sup> For the targeted application presented in Fig. 2, the polymer must be miscible with the solvent in order to enable a homogeneous dispersion of the polymer during the surface functionalisation of  $B_4C$  particles during mixing at room temperature. The solvent was extracted with a rotary evaporator, which implies that a solvent with a low boiling temperature will be preferred. For the sake of recyclability, the polymer-solvent couple that allows for the maximum recovery of each species without degrading them will be chosen. After the preselection of the solvents as an alternative to T,

miscibility tests were performed to testify to the miscibility between the polymer and the solvent. The polymer is miscible with D and C, unlike A. Fig. 3 illustrates the experiments carried out in this study to analyse the interaction between AHPCS and the solvents in contact with it.

This set of experiments aims to investigate the behaviour of the polymer in different solvents, mainly in terms of miscibility and whether the solvent can affect the structure or composition of the polymer. Furthermore, the extraction ability of the polymer will be studied, as well as the potential recyclability of the solvent after polymer extraction. Before and after mixing of the preceramic polymer with the solvent, mass measurements were performed to evaluate the possible losses of polymer and solvent during the process. The amount of AHPCS collected compared to that introduced is lower for each solvent, which reflects a loss of polymer. Polymer yields after extraction are as

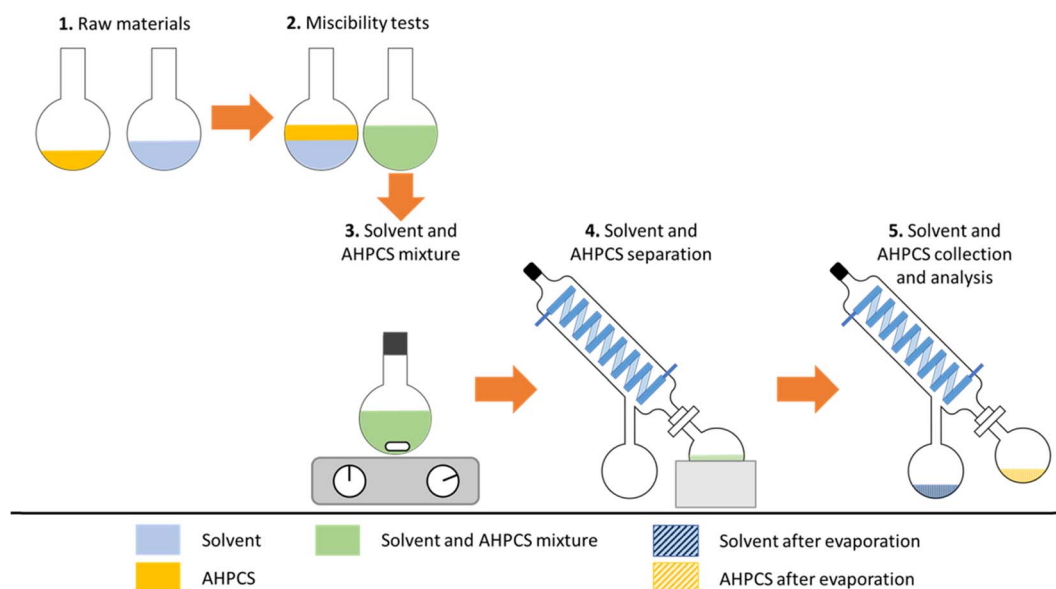


Fig. 3 Experimental plan for analysing the interactions between AHPCS and the solvents in contact with it.





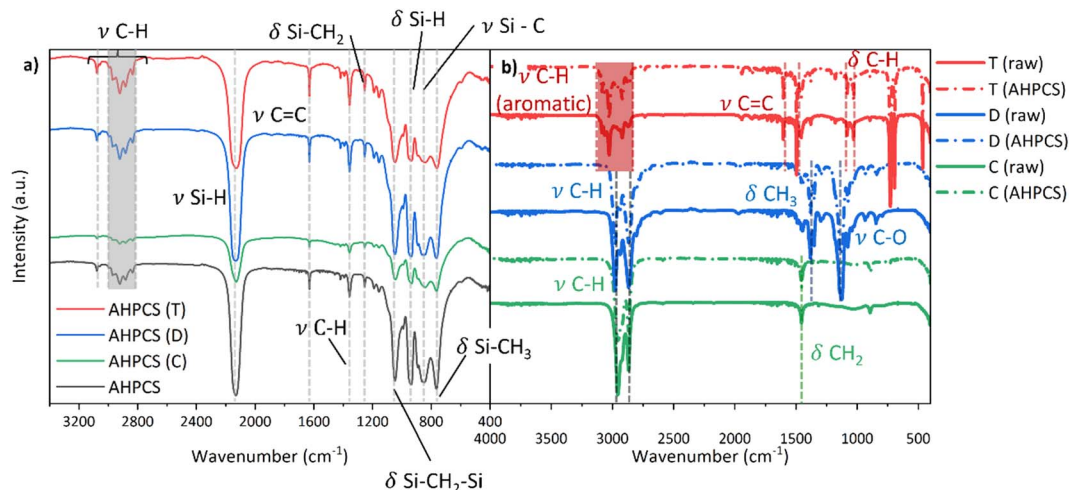


Fig. 4 (a) FT-IR analysis of the polymer before (AHPSCS) and after staying in the solvent; (b) FT-IR analysis of the functionalisation solvent before (raw, full line) and after (dotted line) being in contact with the polymer.

follows: T (92 wt%) < D (97 wt%) < C (99 wt%). This could be explained by the stronger interactions between T and the polymer. Moreover, the heating provided during the evaporation of T could also lead to the evaporation of oligomers present in the polymer, a result confirmed by SEC-MALS analysis. On the other hand, regarding the solvent collected, the mass losses are as follows: D (44 wt%) > C (19 wt%) > T (10 wt%). After collecting the polymer, some structural investigations were performed by

infrared spectroscopy to see whether the contact with the solvent affected its structure. (a) The AHPSCS spectrum shows bands characteristic of the vibrations of polycarbosilane bonds in agreement with the literature.<sup>13,29–31</sup>

After extraction of the solvent, it was interesting to see whether polymer traces could be detected in the solvent. An absence of polymer residues in the solvent could lead to a potential recyclability of the solvent throughout the process.

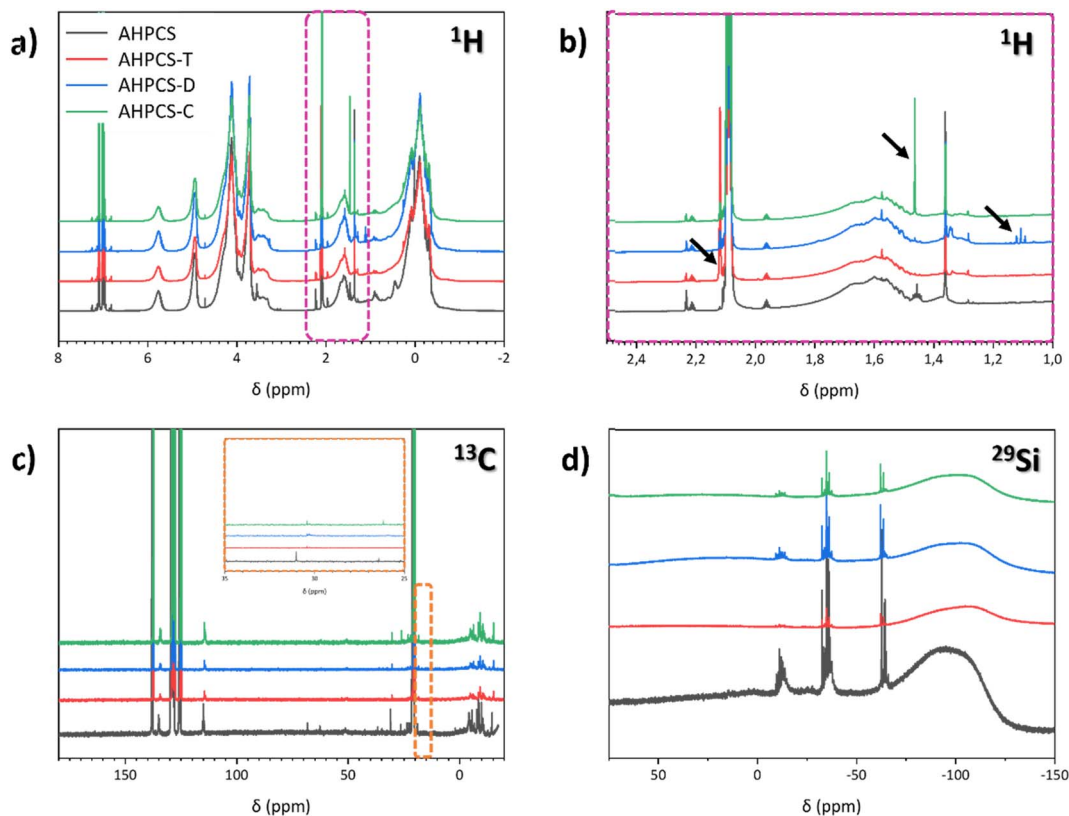


Fig. 5 <sup>1</sup>H (a and b), <sup>13</sup>C (c), and <sup>29</sup>Si (d) NMR analysis of the AHPCS before and after being dissolved in T, D and C.

Fig. 4 presents the IR spectra of the solvent before and after contact with the polymer. The vibration bands typical of each solvent can be observed. However, none of them were attributed to the **AHPCS**. This indicates that there is no detectable amount of polymer in the solvent, and that the solvent could therefore be recycled.

$^1\text{H}$ ,  $^{13}\text{C}$  and  $^{29}\text{Si}$  NMR spectra were also recorded on **AHPCS**, **AHPCS-T**, **D** and **C** (Fig. 5). The  $^1\text{H}$  peaks (Fig. 5a) correspond to what is expected for **AHPCS**, according to the literature.<sup>13,31,32</sup> Some additional small peaks are present (see arrows in Fig. 5b), which are due to some residual solvent (increase of the peak at 2.12 ppm due to the T trace; singlet at 1.46 ppm due to the C residue and triplet at 1.11 ppm due to the D residue). The  $^{13}\text{C}$  NMR spectra were also recorded (Fig. 5c). The signals at 114 and 134 ppm are assigned to the  $\text{CH}=\text{CH}_2$  allyl carbons. Peaks below 0 ppm correspond to  $\text{Si}-\text{CH}_3$  groups, and could be responsible for the presence of free carbon after the polymer pyrolysis.<sup>13,31,33</sup> These spectra are similar to what is expected for **AHPCS**, except for some small peaks between 25 and 35 ppm for **AHPCS-C** due to C residue. As for the  $^{29}\text{Si}$  NMR spectrum of **AHPCS** in Fig. 5d, three chemical shift ranges can be observed due to  $\text{C}_3\text{SiH}$  sites from  $-15$  to  $-8$  ppm, due to  $\text{C}_2\text{SiH}_2$  sites from  $-40$  to  $-30$  ppm, and due to  $\text{CSiH}_3$  sites from  $-67$  to  $60$ .<sup>13,34,35</sup> The spectra of **AHPCS-D**, **AHPCS-T** and **AHPCS-C** are very similar to the previous ones, with a global lower intensity for **AHPCS-T**, which is certainly due to the lower sample concentration. As a conclusion and in line with the IR study, this NMR study ( $^1\text{H}$ ,  $^{13}\text{C}$  and  $^{29}\text{Si}$ ) confirms that the polymer structure is not affected by the presence of any of the three solvents tested.

The thermal behaviour and the ceramic yield of a polymer are of great interest when it comes to sintering. It highlights the suitability of the polymer for use in the sintering process. The thermal behaviour of **AHPCS** was studied before and after contact with the solvent. Results are presented in Fig. 6a. The as-received **AHPCS** presents a ceramic yield of 75% and three

distinct weight loss domains. The first weight loss is observed from  $100^\circ\text{C}$ , the second starts at  $200^\circ\text{C}$ , and the last one at  $450^\circ\text{C}$ . Above  $800^\circ\text{C}$ , no significant weight loss was observed. Mass losses and associated phenomena are in line with expectations according to the literature.<sup>11</sup> MS combined with TGA analysis revealed the departure of different species (Fig. 6b). The first stage of weight loss (4%) was attributed to the departure of oligomers. During the major weight loss (15%) which starts at  $200^\circ\text{C}$ , the reaction of dehydrocoupling took place with the release of hydrogen ( $m/z = 2$ ), and organic fragments ( $m/z = 14$  for  $\text{CH}_2$ ,  $m/z = 15$  for  $\text{CH}_3$ ) were also detected.

In addition, the departure of organic fragments with higher molecular weight ( $m/z = 29$  for  $\text{CH}_3-\text{CH}_2$ ,  $m/z = 31$  for  $\text{CH}_3-\text{OH}/\text{SiH}_3$ ,  $m/z = 43$  for  $\text{C}_3\text{H}_7$  and  $m/z = 44$  for  $\text{C}_3\text{H}_8$ ) was observed, as confirmed by the work of Li *et al.*<sup>30</sup> This main stage was due to the conversion from an organic to inorganic material. Finally, the last weight loss domain (7%) was correlated to the loss of hydrogen ( $m/z = 2$ ) and some organic fragments ( $m/z = 44$  for  $\text{C}_3\text{H}_8$ ). After contact with solvents, the ceramic yields of the polymer slightly decreased compared to the initial value of 75%: 72% for T, D and 73% for C. The second weight loss starting at  $200^\circ\text{C}$  was also different for the polymers in contact with solvents. These characteristics could be due to a loss of oligomers, leading to slightly modified crosslinking.

To elucidate the impact of the process (contact with solvent followed by solvent evaporation) on the molar masses of **AHPCS**, a SEC-MALS analysis was carried out. Fig. 7 displays the elution time of **AHPCS**, and of the different preceramic polymers after the evaporation of the three solvents (**AHPCS-C**, **-D** and **-T**), at a flow rate of  $1\text{ mL min}^{-1}$ . It can be seen that the broad elution profiles changed from **AHPCS** with one maximum of the Rayleigh ratio at roughly  $7.0\text{ mL}$ , to **AHPCS-i**, with two peaks at approximately  $6.0$  and  $6.6\text{ mL}$ . The distillation of the solvents led to an increase of the average molar mass of **AHPCS-i** due to the evaporation of oligomers present in **AHPCS** (Table 2). Thus, even if the molar-mass dispersity remained in the range

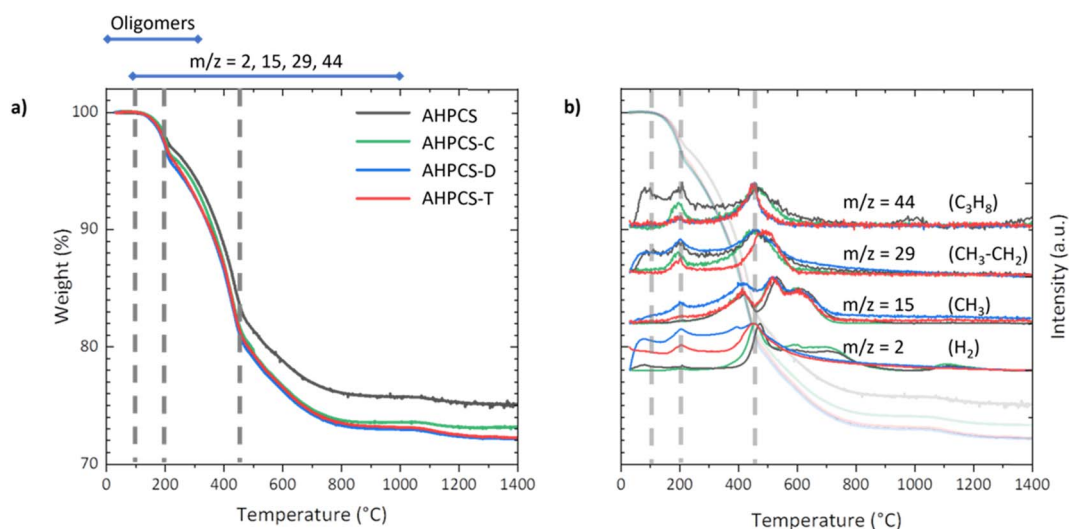


Fig. 6 (a) TGA of the polymer before and after contact with the solvent. (b) Mass spectrometry analysis.



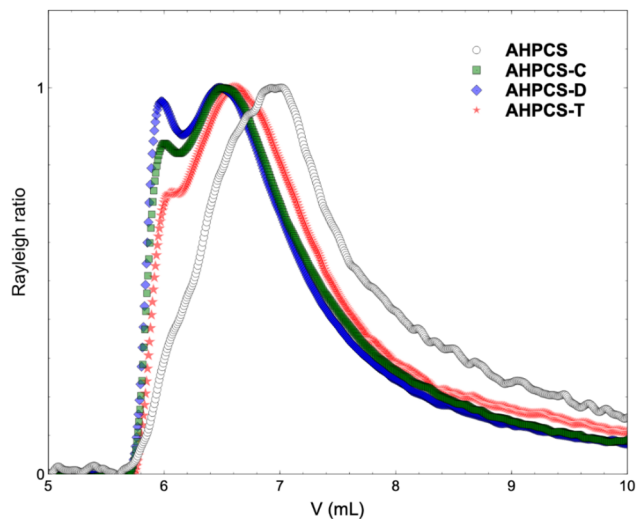


Fig. 7 Chromatograms with SEC-MALS elution profiles of AHPCS and AHPCS-*i* (*i* = C, D or T).

Table 2 Average molar mass ( $\overline{M}_n$ ,  $\overline{M}_w$ ) and molar-mass dispersity ( $D$ ) of AHPCS and recovered AHPCS-*i* (*i* = C, D or T)

	AHPCS	AHPCS-C	AHPCS-D	AHPCS-T
$\overline{M}_n$ (g mol <sup>-1</sup> )	51 510	63 200	63 580	53 070
$\overline{M}_w$ (g mol <sup>-1</sup> )	87 200	126 500	128 600	101 400
$D$	1.7	2.0	2.0	1.9

of 1.7–2.0, AHPCS-D and AHPCS-C had the highest mass-average molar masses at 128 600 and 126 500 g mol<sup>-1</sup>, respectively, while AHPCS-T had a mass-average molar mass that was intermediate between AHPCS and AHPCS-C.

To link these results to the thermal behaviour of the polymers, it seems that the presence of small polymer chains had a slight impact on the final ceramic yield, as the absence of them reduced the ceramic yield by only 2–3%. In summary, the polymer structure did not seem to be affected by the change of solvent, and AHPCS recycling could also be considered feasible at the end of the process.

### Application to B<sub>4</sub>C functionalisation

B<sub>4</sub>C and SiC are non-oxide ceramics commonly used for their low density, combined with a high hardness and good chemical stability. The preparation of B<sub>4</sub>C/SiC composites by powder mixing and sintering has already been investigated. However, this method of making composites still faces certain drawbacks, such as chemical inhomogeneities, contamination due to milling steps, leaching steps necessary to remove impurities, or higher sintering temperatures.

The preparation of a composite *via* the PDC route is an alternative that allows for overcoming these drawbacks,<sup>11</sup> and was used here to make B<sub>4</sub>C/SiC (AHPCS) composites. The influence of the nature of the solvent on the PDC route was studied. Fig. 2 illustrates the protocol used to produce the B<sub>4</sub>C/SiC specimens by spark plasma sintering (SPS).

B<sub>4</sub>C powders were studied by transmission electron microscopy (TEM) before and after mixing with AHPCS in solvent, as presented in Fig. 8. Before mixing, B<sub>4</sub>C particles present a native amorphous layer of boron hydroxide (H<sub>3</sub>BO<sub>3</sub>),<sup>36</sup> identified with dotted line, that is less than 5 nm thick. After mixing with the polymer in the presence of a solvent, a thicker amorphous layer can be observed that is up to 10 nm thick, depending on the particle geometry. X-ray photoelectron spectroscopy (XPS) experiments (*cf.* ESI†) reveal the presence of Si in this amorphous layer, which confirms the presence of AHPCS at the

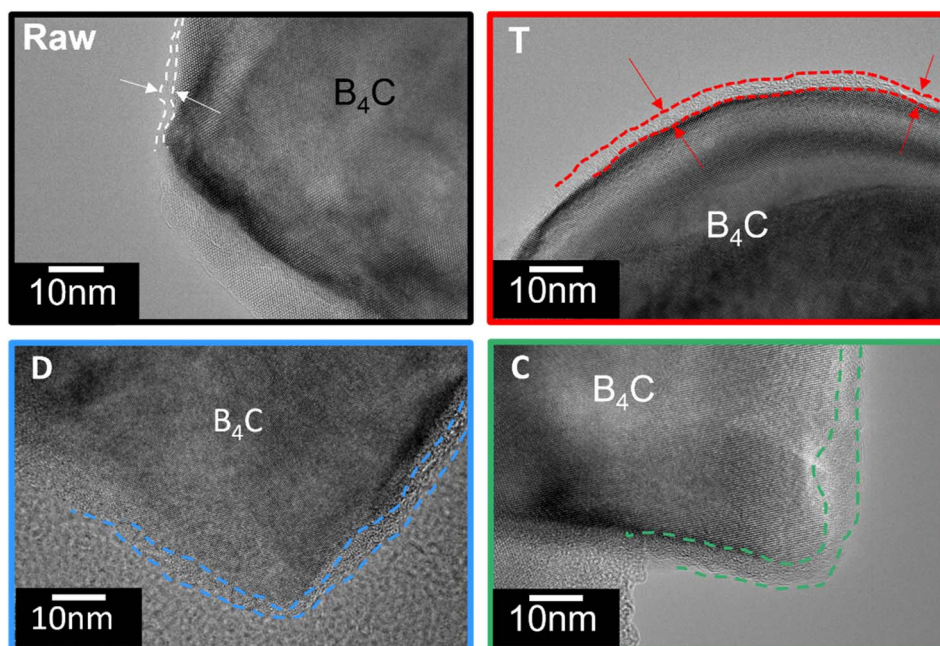


Fig. 8 TEM images of boron carbide powder before (raw) and after functionalisation in different solvents: T, D or C.



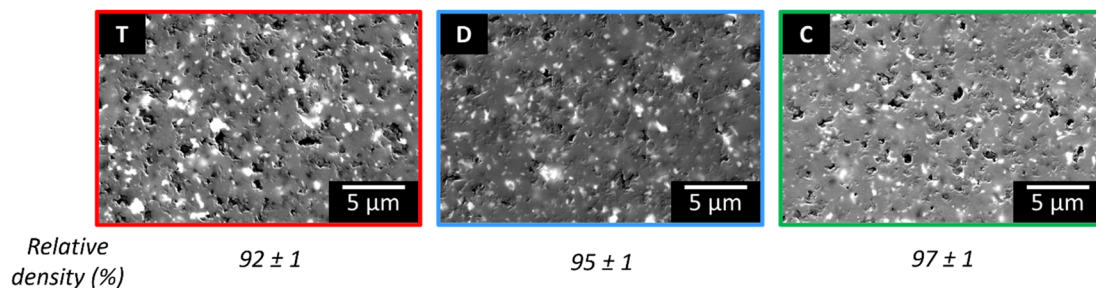


Fig. 9 SEM (back-scattered electrons) observations of the sintered specimens after functionalisation in T, D or C. The dark grey phase corresponds to  $B_4C$  and the light grey to  $\beta$ -SiC.

particle surface. Owing to the interactions (chemical or physical) that can be developed between the polymer and the particles in the presence of the solvent, the polymer is dispersed and deposited homogeneously, leading to the surface functionalisation of the  $B_4C$  particles.

The sinterability of  $B_4C/AHPCS$  was investigated using SPS, a non-conventional sintering technique in which densification is assisted by uniaxial pressure and heating by Joule effect with a current flowing through the sample. The specimens were subjected to the same thermomechanical sintering cycle that had been optimised in previous studies.<sup>24</sup> The sintering steps were adapted in order to achieve an *in situ* conversion of the polymer from organic to inorganic, followed by the sintering step. The relative density of the specimens was slightly different depending on the functionalisation solvent (92% for T, 95% for D and 97% for C).<sup>11</sup> This result could be explained by a modification of the surface potential depending on solvent, resulting in an agglomeration state of grains. The relative densities obtained are above 90%, which was the lower limit targeted in this study. For refractory or abrasive applications, a minimum relative density is required to achieve the mechanical properties required for the application. Moreover, the comparison of the microstructures of the samples, shown in Fig. 9, did not reveal any major differences regardless of what solvent was used. According to XRD analysis, the phases present in each case are  $B_4C$  (dark grey) and  $\beta$ -SiC (light grey), as well as residual carbon (no visible) due to the non-stoichiometric Si/C ratio of the starting polymer. The samples can be described as a fine dispersion of  $\beta$ -SiC within the  $B_4C$  matrix, with the presence of residual porosity.

## Conclusions

This study aimed to find a replacement solvent for the processing of  $AHPCS$ , a preceramic polycarbosilane. An approach was developed to study the interactions between the solvent and the polymer, and the possible effects on its structure and processing. Two solvents, diethyl ether (D) and cyclopentane (C), were found to be good alternatives to toluene (T) both in terms of safety and for the targeted application, which was the surface functionalisation of the  $B_4C$  particles to prepare  $B_4C/SiC$  composites. However, according to some risk ranking,<sup>37,38</sup> C would rather be chosen than D. These new solvents did not

affect the polymer structure, as confirmed by  $^1H$ ,  $^{13}C$  and  $^{29}Si$  NMR, as well as FT-IR (ATR) analysis. The polymer ceramic yield slightly decreased by only a few percent after contact with the solvent, which is certainly due to a loss of small oligomers. The thermal behaviour of the polymer can therefore be considered unaffected by the change of solvent. This set of results highlights the recyclability of the polymer, which is not affected by the solvent.

On the other hand, FT-IR (ATR) characterisation of the solvent, before and after contact with the polymer, revealed no major polymer residue. In the context of the process industrialisation, this result means that the solvents can be recycled.

With regard to the targeted application, the solvent used for the functionalisation of  $B_4C$  particles did not affect the final result. The type of interactions which are involved in the deposition of the polymer at the surface of  $B_4C$  particles is not yet identified, and is still under investigation with complementary NMR and XPS investigations. The functionalisation using C gives the best relative density (97%) of the sintered  $B_4C/SiC$  composites compared to D-(95%) and T-(92%). Indeed, the solvent did not affect the functionalisation step. The variation in relative density was attributed to the sintering step.

## Data availability

The data supporting this article have been included as part of ESI.†

## Author contributions

The manuscript was written through the contributions of all authors.

## Conflicts of interest

There are no conflicts to declare.

## Acknowledgements

The authors wish to thank Baptiste Rigaud for his helpful assistance for liquid NMR. The research study was funded by the Ministry of Defence – Defence Innovation Agency. This work





is supported by institutional grants from the National Research Agency under the Investments for the future program with the reference ANR-18-EURE-0017 TACTIC.

## Notes and references

- 1 D. Demirskyi, H. Borodianska, Y. Sakka and O. Vasylykiv, *J. Eur. Ceram. Soc.*, 2017, **37**, 393.
- 2 R. Belon, G. Antou, N. Pradeilles, A. Maître and D. Gosset, *Ceram. Int.*, 2017, **43**, 6631.
- 3 B. J. Ackley, K. L. Martin, T. S. Key, C. M. Clarkson, J. J. Bowen, N. D. Posey, J. F. Ponder Jr, Z. D. Apostolov, M. K. Cinibulk and T. L. Pruyn, *Chem. Rev.*, 2023, **123**, 4188.
- 4 D. Schawaller and B. Claus, *High Temp. Ceram. Matrix Compos.*, 2001, 56–61.
- 5 H. Xiong, L. Zhao, H. Chen, H. Luo, X. Yuan, K. Zhou and D. Zhang, *J. Eur. Ceram. Soc.*, 2021, **41**, 1121.
- 6 R. Lörcher, K. Strecker, R. Riedel, R. Telle and G. Petzow, *Solid State Phenom.*, 1991, **8–9**, 479.
- 7 R. Chen, A. Bratten, J. Rittenhouse, M. Leu and H. Wen, *J. Am. Ceram. Soc.*, 2023, **106**, 4028–4037.
- 8 M. Kubo, M. Kojima, R. Mano, Y. Daiko, S. Honda and Y. Iwamoto, *J. Membr. Sci.*, 2020, **598**, 117799.
- 9 R. A. Wach, M. Sugimoto and M. Yoshikawa, *J. Am. Ceram. Soc.*, 2007, **90**, 275.
- 10 S. Chakraborty, D. Debnath, A. R. Mallick, R. K. Gupta, A. Ranjan, P. K. Das and D. Ghosh, *Int. J. Refract. Met. Hard Mater.*, 2015, **52**, 176.
- 11 H. Laadoua, N. Pradeilles, R. Lucas, S. Foucaud and W. J. Clegg, *J. Eur. Ceram. Soc.*, 2020, **40**, 1811.
- 12 M. Bougoin and F. Thevenot, *J. Mater. Sci.*, 1987, **22**, 109.
- 13 R. Sreeja, B. Swaminathan, A. Painuly, T. V. Sebastian and P. Shanmugam, *Mater. Sci. Eng., B*, 2010, **168**, 204.
- 14 S. Kaur, R. Riedel and E. Ionescu, *J. Eur. Ceram. Soc.*, 2014, **34**, 3571.
- 15 R. P. Chaudhary, C. Parameswaran, M. Idrees, A. S. Rasaki, C. Liu, Z. Chen and P. Colombo, *Prog. Mater. Sci.*, 2022, **128**, 100969.
- 16 M. Pelanconi, G. Bianchi, P. Colombo and A. Ortona, *J. Am. Ceram. Soc.*, 2022, **105**, 786.
- 17 G. D. Soraru, F. Dalcanale, R. Campostrini, A. Gaston, Y. Blum, S. Carturan and P. R. Aravind, *J. Mater. Chem.*, 2012, **22**, 7676.
- 18 K. König, V. Boffa, B. Buchbjerg, A. Farsi, M. L. Christensen, G. Magnacca and Y. Yue, *J. Membr. Sci.*, 2014, **472**, 232.
- 19 C. M. Hansen, *Hansen Solubility Parameters: a User's Handbook*, CRC press, 2007.
- 20 S. Abbott and C. M. Hansen, *Hansen Solubility Parameters in Practice*, Hansen-Solubility, 2008.
- 21 F. Byrne, B. Forier, G. Bossaert, C. Hoebers, T. J. Farmer, J. H. Clark and A. J. Hunt, *Green Chem.*, 2017, **19**, 3671.
- 22 Q. Wang, M. Yokoji, H. Nagasawa, L. Yu, M. Kanezashi and T. Tsuru, *J. Membr. Sci.*, 2020, **612**, 118392.
- 23 C. Hwang, Q. Yang, S. Xiang, V. Domnich, A. U. Khan, K. Y. Xie, K. J. Hemker and R. A. Haber, *J. Eur. Ceram. Soc.*, 2019, **39**, 718.
- 24 L. Roumiguier, A. Jankowiak, N. Pradeilles, G. Antou and A. Maître, *Ceram. Int.*, 2019, **45**, 9912.
- 25 J. K. Fink, in *Petroleum Engineer's Guide to Oil Field Chemicals and Fluids*, ed. J. K. Fink, Gulf Professional Publishing, Boston, 2012, pp. 663–694, DOI: [10.1016/B978-0-12-383844-5.00021-0](https://doi.org/10.1016/B978-0-12-383844-5.00021-0).
- 26 B. Zhuang, G. Ramanauskaitė, Z. Y. Koa and Z.-G. Wang, *Sci. Adv.*, 2021, **7**, eabe7275.
- 27 C. Higginbotham, *Introductory Organic Chemistry*, 2021.
- 28 Cymit Quimica, 2,2,5,5-Tetramethyloxolane, <https://cymitquimica.com/fr/produits/3D-FT172401/15045-43-9/2255-tetramethyloxolane/>, accessed 09/01/2024, 2024.
- 29 Z. Yu, L. Yang, J. Zhan, C. Zhou, H. Min, Q. Zheng and H. Xia, *J. Eur. Ceram. Soc.*, 2012, **32**, 1291.
- 30 H. Li, L. Zhang, L. Cheng, Y. Wang, Z. Yu, M. Huang, H. Tu and H. Xia, *J. Eur. Ceram. Soc.*, 2008, **28**, 887.
- 31 Y. Fang, M. Huang, Z. Yu, H. Xia, L. Chen, Y. Zhang and L. Zhang, *J. Am. Ceram. Soc.*, 2008, **91**, 3298.
- 32 M. Huang, Y. Fang, R. Li, T. Huang, Z. Yu and H. Xia, *J. Appl. Polym. Sci.*, 2009, **113**, 1611.
- 33 C. Stabler, E. Ionescu, M. Graczyk-Zajac, I. Gonzalo-Juan and R. Riedel, *J. Am. Ceram. Soc.*, 2018, **101**, 4817.
- 34 Z. Yu, M. Huang, Y. Fang, R. Li, J. Zhan, B. Zeng, G. He, H. Xia and L. Zhang, *React. Funct. Polym.*, 2010, **70**, 334.
- 35 S. Park, D.-H. Lee, H.-I. Ryoo, T.-W. Lim, D.-Y. Yang and D.-P. Kim, *Chem. Commun.*, 2009, 4880.
- 36 F. Réjasse, M. Georges, N. Pradeilles, G. Antou and A. Maître, *J. Am. Ceram. Soc.*, 2018, **101**, 3767.
- 37 M. Tobiszewski, S. Tsakovski, V. Simeonov, J. Namieśnik and F. Pena-Pereira, *Green Chem.*, 2015, **17**, 4773.
- 38 D. Prat, J. Hayler and A. Wells, *Green Chem.*, 2014, **16**, 4546.

